

RPT: Learning Point Set Representation for Siamese Visual Tracking

Ziang Ma, Linyuan Wang, Haitao Zhang, Wei Lu, and Jun Yin

Zhejiang Dahua Technology, Hangzhou, China

{ma_ziang,wang_linyuan,zhang_haitao1,lu_wei,yin_jun}@dahuatech.com

Abstract. While remarkable progress has been made in robust visual tracking, accurate target state estimation still remains a highly challenging problem. In this paper, we argue that this issue is closely related to the prevalent bounding box representation, which provides only a coarse spatial extent of object. Thus an efficient visual tracking framework is proposed to accurately estimate the target state with a finer representation as a set of representative points. The point set is trained to indicate the semantically and geometrically significant positions of target region, enabling more fine-grained localization and modeling of object appearance. We further propose a multi-level aggregation strategy to obtain detailed structure information by fusing hierarchical convolution layers. Extensive experiments on several challenging benchmarks including OTB2015, VOT2018, VOT2019 and GOT-10k demonstrate that our method achieves new state-of-the-art performance while running at over 20 FPS.

Keywords: Visual tracking, Point set representation, Mutil-level aggregation

1 Introduction

Robust visual tracking is a fundamental task for various computer vision applications, including video monitoring analysis, man-machine interaction and intelligent driving. It aims at locating an arbitrary target of interest during a whole video sequence. Although substantial progress has been made in recent years, the design of a high-performance tracker is still highly challenging due to moving camera, occlusions and variations in structure.

Much attention has been invested for accurately estimating the target state in recent years. Its difficulty lies in frequently changed appearance caused by target or camera movement and varying postures. A region proposal network (RPN) was introduced to estimate the target bounding box with a pre-defined set of anchor boxes [16,15,38]. However, it hinders the generalization and efficiency of the Siamese-based tracking framework. The no-prior box design was subsequently presented [32,3,8], which is free of prior knowledge about target scale/ratio distribution. It directly views locations as training samples and predicts the relative offsets to the corners or sides of bounding box. The location is

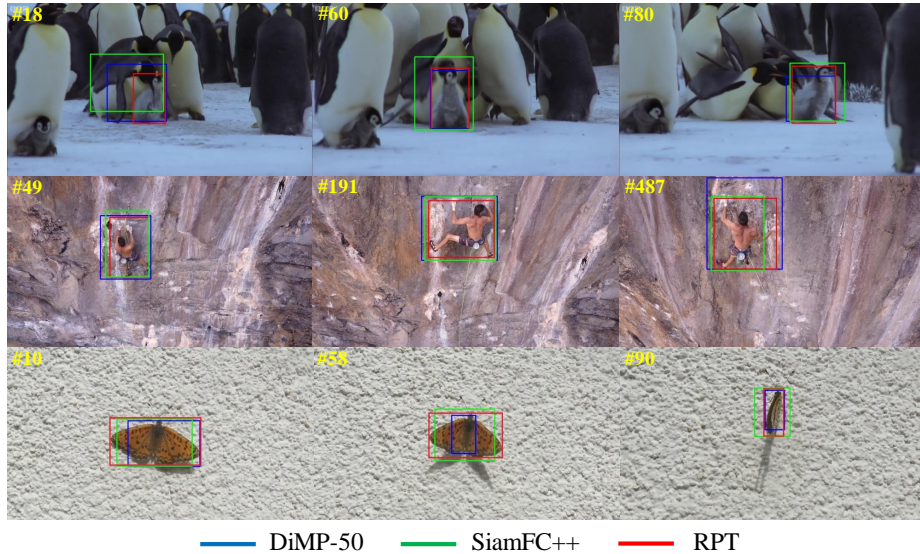


Fig. 1. Qualitative comparisons with state-of-the-art trackers. Our approach RPT obtains more accurate bounding box predictions when handling variations in posture, scale and aspect ratio

assigned with a positive label if it falls within a preset center area of the ground-truth bounding box, ignoring the target appearance and geometric structure. Besides, the target state is commonly described with a bounding box for the conveniences of feature extraction and ground truth annotation. It provides only a coarse spatial extent of object, and lacks the modeling capability for geometric transformations, thereby severely restricting the localization accuracy [33,34].

In this paper, we propose a novel tracking method named Representative Points based Tracker (RPT) to address the issue of accurate target estimation. RPT models the target state with a new finer representation as a set of representative points, and learns to arrange them to indicate the target’s spatial extent and geometrically significant positions. In contrast to the coarse encoding of bounding box, the point set representation facilitates more fine-grained localization and modeling of object appearance. The RPT framework is constructed with two parallel branches, one primarily accounting for target estimation with the point set representation, the other trained online to provide high robustness against distractors.

The main contributions of this paper are threefold.

- A novel point set representation facilitating more accurate target estimation is employed in the field of visual tracking.
- We aggregate hierarchical convolution layers to provide detailed structural information of target and high discriminative power when handling distractors.

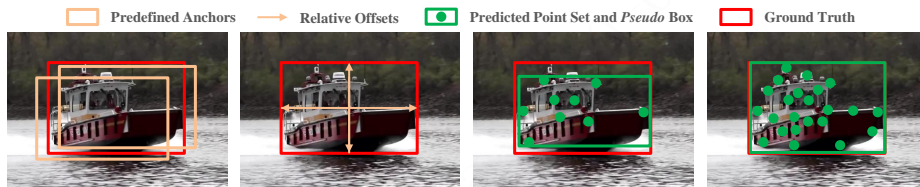


Fig. 2. Comparison for methods used to estimate the target state. Multi-level aggregation provides detailed structure information of objects, facilitating more fine-grained localization

- Our work achieves new state-of-the-art performances and runs at 20 FPS on several benchmarks, including OTB2015 [30], VOT2018 [14], VOT2019 [13] and GOT-10k [12].

2 Related Work

Visual tracking is a fundamental computer vision problem, which can be divided into a foreground-background classification task and a target state estimation task. The former case is responsible for distinguishing the target appearance from distractors and the surrounding background. The latter one aims to accurately describe the target region against variations in posture, scale and aspect ratio.

Discriminative correlation filters [7,22,27] and online learning approaches [6,37] have remarkably advanced the target classification task in recent years. On the other hand, accurately estimating the target state is still challenging and severely limited with a multi-scale search strategy [11,5,1,27]. The target state is usually represented with a bounding box, and further estimated with various methods. SAMF[17] adopts a multiple scales searching strategy to address the issue of scale variations. GOTURN[10] designs a box regression strategy with the Laplace distribution hypothesis, which is restricted to small motions and limited scale changes. SiamRPN and the succeeding works [16,15,38] introduce a region proposal network (RPN) to regress the target region from pre-defined anchors. It leads to an apparent degeneration in tracking efficiency and generalization. ATOM [6] iteratively refines the coarse initial location to obtain a higher overlap between the predicted bounding box and ground truth. Inspired from anchor-free detection pipeline, a no-prior box design is utilized to predict offsets from candidate locations to the corners or sides of desired bounding box [32,3,8].

In order to describe more spatial details of objects, rotated bounding box and segmentation mask are further utilized to represent the target state in visual tracking [18,29,21]. LDES simultaneously estimates the orientation and scale variation of target via polar coordinate transformation [18]. SiamMask produces a binary segmentation mask via an extra branch trained on YouTube-VOS[31], which is a large video dataset with pixel-wise annotations [29]. D3S obtains a noticeable advancement in segmentation accuracy by constructing a parallel structure with complementary geometric models [21].

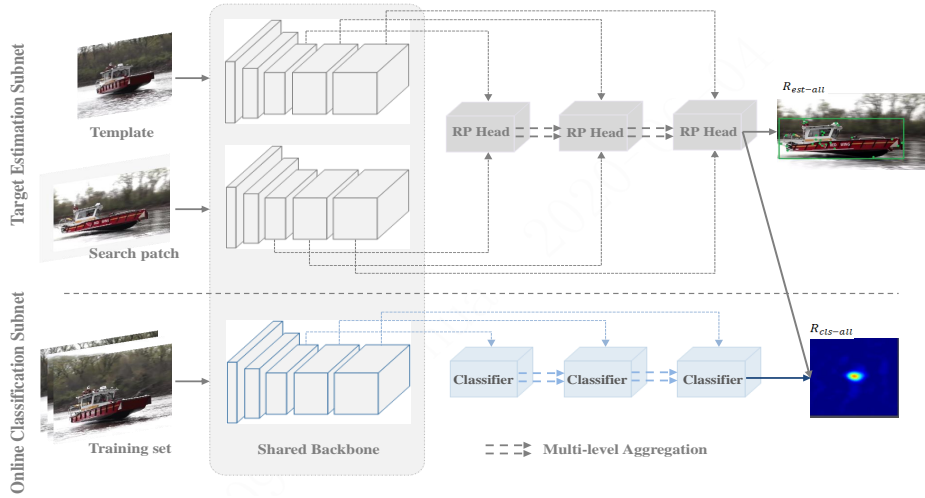


Fig. 3. The RPT framework with multi-level aggregation. The target estimation subnet predicts the spatial extent of object with a set of representative points in an offline-trained embedding space. The online classification subnet is responsible for distinguishing the target appearance from distractors and the surrounding background

3 RPT Framework

The RPT framework is constructed with a shared backbone network for feature extraction, and two parallel subnets accounting for target estimation and online classification respectively, as illustrated in Figure 3. Following the architectural design guidelines in [36], we adopt ResNet-50 [9] as the backbone network, and extract hierarchical convolutional features from the last three residual blocks for multi-level prediction. The target estimation subnet is driven by a finer representation of object as a point set, which provides more fine-gained localization. The online classification subnet is trained exclusively online to enhance the discriminative capability in the presence of distractors.

3.1 Target Estimation with Point Set Representation

In contrast to object detection, tracking target can be an arbitrary object with unknown class. We therefore exploit Siamese-based feature extraction and matching for the requirement of target-specific estimation. Multi-level features from a target template (denoted as z) and a search region (denoted as x) are extracted. For each feature level, a correlation map between the target patch and the search patch is obtained via depth-wise cross correlation [15] as:

$$g_l(z, x) = \varphi_l(z) * \varphi_l(x) \quad (1)$$

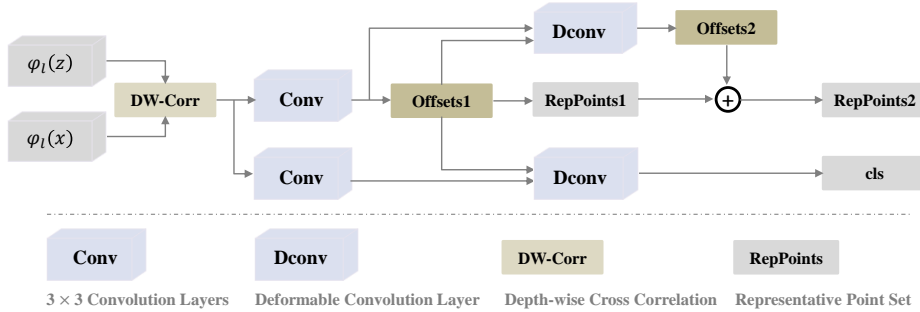


Fig. 4. The architecture of RP Head

where $\varphi_l(z)$ and $\varphi_l(x)$ represent the corresponding feature outputs of the l -th level.

Inspired from [33], we design a classification head and a two-stage regression head over the correlation map. The head architecture is illustrated in Figure 4. Each location of the correlation map is regarded as a target candidate. For the location (i, j) , the target state is modeled with a set of sample points, which are uniformly initialized with the corresponding position as:

$$R = \{(x_k, y_k)\}_{k=1}^n \quad (2)$$

$$x_k = i, y_k = j, k = 1, 2, \dots, n \quad (3)$$

where n represents the capacity of the point set. For each candidate, the regression head outputs a set of offsets to refine the distribution of sample points, while the classification head outputs two-channels for foreground-background classification. Specifically, the initial sample points are progressively refined with extra offsets in a point-wise manner:

$$R_r = \{(x_k + \Delta x_k, y_k + \Delta y_k)\}_{k=1}^n \quad (4)$$

where the predicted offsets $\{(\Delta x_k, \Delta y_k)\}_{k=1}^n$ are paired with the deformable convolution [4]. In contrast to its standard counterpart, deformable convolution augments the regular spatial sampling locations with additional offsets. It has the capability of modeling various geometric transformations for scale, aspect ratio and rotation. The kernel size of deformable convolutions is commonly set as 3×3 . The number of representative points n is accordingly set to 9 in this work.

The refinement process is offline-trained with a multi-task loss for simultaneous localization and recognition. In the field of visual tracking, the target region is usually annotated with a bounding box, which is inconsistent with the point

set representation. In order to utilize the bounding box annotations for supervision, we perform a min-max operation over the refined point set obtaining a pseudo box as:

$$B_p = (\min \{x_k + \Delta x_k\}, \min \{y_k + \Delta y_k\}, \max \{x_k + \Delta x_k\}, \max \{y_k + \Delta y_k\}) \quad (5)$$

In our work, the ratio of the overlapping area between the induced pseudo box and ground-truth bounding box to the union area is utilized to represent the regression loss. The focal loss [19] focusing on hard examples is further employed for foreground-background classification. Driven by both target regression and classification losses, a set of representative points are automatically learned that indicates the object boundaries and semantically prominent regions.

3.2 Discriminative Online Classification

The classification head discussed above is employed to distinguish foreground from background. However, it lacks the capacity to discriminate the target object from similar surrounding instances. In this section, we propose to complement the target estimation pipeline with an online-trained classifier to provide high robustness against distractors. Similar to [6,37], it is modeled as a light weight 2-layer fully convolutional neural network for efficiency.

The online classifier is trained with a certain amount of target regions obtained from the last few frames, which share the same size to the search patch. The training sample is commonly labeled with a two-dimensional Gaussian function centered at the target position, where the geometric structure of object is neglected. Here, we propose to label the confidence of target presence according to the representative point set. It is offline-learned to indicate the spatial extent of object and semantic key points. The desired classification score for each pixel of the training sample is therefore constructed by calculating the average position deviation to the point set.

After obtaining the online classification score, we combine it with the classification head output of the target estimation subnet as

$$f_l = \alpha f_{online}^l + (1 - \alpha) f_{offline}^l \quad (6)$$

where f_*^l represents the corresponding response maps for the l -th level, and α is the parameter controlling the impact of these two confidence scores.

3.3 Multi-level Aggregation

As pointed by [24,23], convolutional features extracted from earlier layers preserve finer spatial information benefiting for precise localization, while latter activations capture rich semantic information facilitating robustness against variation in appearance. Thus we propose to employ hierarchical convolutional layers contributing to the inference of both online classification and target estimation.

For online classification, the per-pixel confidences of target presence obtained from each classifier are combined via a weighted-fusion layer as

$$R_{cls-all} = \sum_{l=3}^5 w_l * f_l \quad (7)$$

The outputs of the last three residual blocks share the same spatial resolution, weighted sum is therefore implemented in a pixel-wise manner. The set of weights w_l are end-to-end optimized together with the network.

For the target estimation subnet, each head outputs only a small set of representative points, which are insufficient when handling complicated object structures. Tracking accuracy is also limited as an inaccurate pseudo box is obtained from the sparse point set. Thus we propose to utilize a significantly larger set of points as the target state representation. The dense point set is simply constructed as a collection of representative points obtained by each head:

$$R_{est-all} = \bigcup_{l=3}^5 R_l, \quad R_l = \{(x_k^l, y_k^l)\}_{k=1}^n \quad (8)$$

As shown in Figure 2, the fusion of sample points provides more elaborate structure of objects that is beneficial for accurate target estimation.

4 Experiments Results

4.1 Implementation Details

Following the architectural design guidelines in [36], ResNet-50 [9] pre-trained on ImageNet [26] is adopted as our backbone network. Multi-level features from the last three residual blocks are extracted for aggregation. The down-sampling operations are removed in the *conv4* and *conv5* blocks to preserve finer spatial information. Meanwhile, dilated convolutions with different atrous rates are exploited to improve the receptive fields.

The target estimation subnet is trained offline with image pairs selecting from YouTube-BoundingBox [25], COCO [20] and ImageNet VID [26]. For the first stage regression, location (i, j) on the correlation map is considered as a positive sample if its corresponding location on the search region is closest to the center of tracking target. The second stage regression and classification are then conducted on the first set of representative points. If the IOU (intersection-over-union) between the induced pseudo box and ground-truth is larger than 0.5, it is assigned with a positive label, and if the IOU is smaller than 0.4, it is assigned with a negative label, and otherwise ignored. For both stages, only the positive samples are exploited for the target state regression.

The training process is driven by SGD on 8 GPUs with 128 image pairs per mini-batch for 20 epochs. We employ a warm-up learning rate linearly ascended

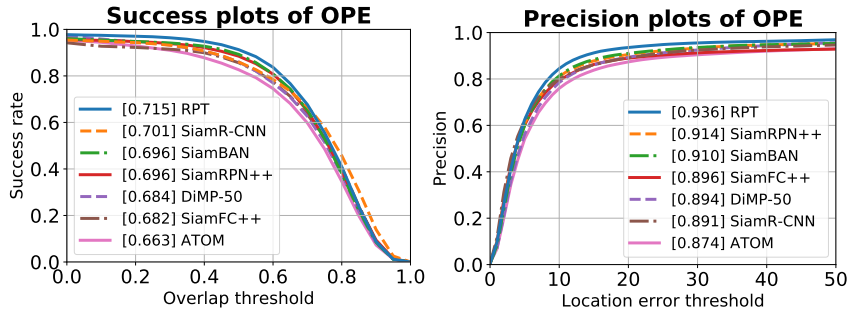


Fig. 5. Success and precision plots on OTB2015

from 0.001 to 0.005 for the first 5 epochs, while the learning rate for the last 15 epochs is exponentially decayed from 0.005 to 0.0005. In the first 10 epochs, only the head architecture of target estimation is trained. The whole network is fine-tuned in the last 10 epoch, where the learning rate of backbone is set to be 10 times smaller than the base value. The online classification subnet is trained with target regions obtained from the last few frames. Conjugate Gradient [6] is employed as the optimizer for efficient online learning. Our tracker is implemented on a PC with a GeForce GTX 1080Ti GPU using PyTorch.

4.2 Comparison with SOTA

The proposed RPT is compared with state-of-the-art trackers on several popular tracking Benchmarks, including OTB2015 [30], VOT2018 [14], VOT2019 [13] and GOT-10k [12].

OTB2015. OTB2015 [30] is one of the most widely used datasets for quantitative evaluation in visual tracking. We compare RPT with numerous recent and advanced visual trackers, including SiamRPN++ [15], ATOM [6], DiMP [2], SiamFC++ [32], SiamR-CNN [28] and SiamBAN [3], in terms of precision score and success rate. The precision score is formulated as the fraction of frames where the distance from the center of tracking result to the ground truth is under 20 pixels, while the success rate denoted as the proportion of frames whose intersection-over-union with the ground truth surpasses 0.5. As illustrated in Figure 5, our tracker obtains an AUC (area under curve of success plot) score of 0.715 and precision score of 0.936, which are 1.4 and 2.2 percentage points higher than the previous best result of SiamR-CNN [28] and SiamRPN++ [15].

GOT-10k. GOT-10k [12] is a large-scale dataset for tracking evaluation, which contains almost over 10 thousand sequences in training subset and 180 sequences in both validation and test subsets. Average overlap (AO) is employed for evaluations on this benchmark. For fair comparison, methods are required to be trained using the given dataset. The proposed RPT achieves a competitive result compared with the state-of-the-art methods with an AO score of 0.624, as shown in Table 1.

Table 1. Comparison with state-of-the-art trackers on GOT-10k. The best two results are marked in red and blue fonts

	ATOM [6]	SiamFC++ [32]	D3S [21]	DiMP-50 [2]	SiamR-CNN [28]	RPT
$SR_{0.5}(\uparrow)$	0.635	0.695	0.676	0.717	0.728	0.730
$SR_{0.75}(\uparrow)$	0.402	0.479	0.462	0.492	0.597	0.504
AO(\uparrow)	0.556	0.595	0.597	0.611	0.649	0.624

VOT2018. VOT2018 [14] consists of 60 sequences with various challenging factors. In contrast to the aforementioned datasets, it's annotated with a rotated bounding box and restarted the tracker in case of failures. Methods are measured with three evaluation metrics, namely accuracy (A), robustness (R) and expected average overlap (EAO). Table 2 shows the comparison with the existing top-performing approaches on VOT2018 [14], in which RPT attains the best robustness and EAO among all methods. D3S [21] is superior in terms of accuracy as numerous segmentation sequences from Youtube-VOS [31] are utilized to produce a binary mask.

VOT2019. VOT2019 [13] is refreshed by replacing the 12 least difficult sequences from the previous version with several carefully selected sequences in GOT-10k dataset. The same measurements are exploited for performance evaluation. As illustrated in Table 2, we achieve an accuracy of 0.623, a robustness of 0.186 and an EAO of 0.417, outperforming DRNet [13] (leading performance on the public dataset of VOT2019 challenge) and other SOTA methods in terms of all metrics.

Table 2. Comparison with state-of-the-art trackers on VOT2018 and VOT2019. The best two results are marked in red and blue fonts

	VOT2018			VOT2019		
	EAO(\uparrow)	R(\downarrow)	A(\uparrow)	EAO(\uparrow)	R(\downarrow)	A(\uparrow)
ATOM [6]	0.401	0.204	0.590	0.292	0.411	0.603
SiamR-CNN [28]	0.408	0.220	0.609	-	-	-
SiamRPN++ [15]	0.414	0.234	0.600	0.285	0.482	0.599
SiamFC++ [32]	0.426	0.183	0.587	-	-	-
DiMP-50 [2]	0.440	0.153	0.597	0.379	0.278	0.594
SiamBAN [3]	0.452	0.178	0.597	0.327	0.396	0.602
SiamAttn [35]	0.470	0.160	0.630	-	-	-
DRNet [13]	-	-	-	0.395	0.261	0.605
D3S [21]	0.489	0.150	0.640	-	-	-
RPT	0.510	0.103	0.629	0.417	0.186	0.623

4.3 Ablation Study

In this section, an extensive ablation study is conducted to verify the impact of individual components on OTB2015 [30]. The modified version of SiamFC++ [32] using ResNet-50 [9] as backbone network is exploited as baseline. As illustrated in Table 3, the baseline approach obtains an AUC score of 0.675. By gradually adding the components of point set representation, online classification and multi-level aggregation, we achieve sustained performance gains of 2.5%, 0.9% and 0.6% in terms of AUC score. It is proven that the main contributions of our work facilitate more accurate target estimation. A similar conclusion can be obtained on other benchmarks.

Table 3. Ablation Study on OTB2015. Baseline denotes a modified SiamFC++ with ResNet-50 as backbone. PSR, OC and MLA represent the components of point set representation, online classification and multi-level aggregation, respectively

Baseline	PSR	OC	MLA	Precision(\uparrow)	AUC(\uparrow)	Δ AUC
\checkmark	\times	\times	\times	0.898	0.675	-
\checkmark	\checkmark	\times	\times	0.925	0.700	+2.5%
\checkmark	\checkmark	\checkmark	\times	0.928	0.709	+0.9%
\checkmark	\checkmark	\checkmark	\checkmark	0.936	0.715	+0.6%

4.4 Evaluation on VOT2020 Challenge

In contrast to previous versions, VOT2020 is annotated with segmentation masks using a new performance evaluation protocol. The novel protocol avoids tracker-dependent resets and re-defines the VOT basis measures. For evaluations on segmentation, the RPT framework is complemented with a modified D3S [21] to obtain class-agnostic object mask. In particular, the target location channel in D3S [21] is enhanced with the average position deviations from the representative point set. The augmented version of RPT achieves an EAO of 0.539 on VOT2020 challenge.

5 Conclusions

In this paper, we propose a novel tracking architecture named RPT to accurately estimate the target state with a finer point set representation. The RPT framework consists of two parallel branches, one primarily accounting for accurate target state estimation in an offline-trained embedding space, the other trained online to obtain high discriminative power in the presence of distractors. Besides, multiple convolution layers are aggregated to provide more fine-grained localization and detailed structural information of target. Comprehensive evaluations on various visual tracking datasets indicate that our method outperforms the recent and advanced trackers in terms of robustness and accuracy.

References

1. Bertinetto, L., Valmadre, J., Henriques, J.F., Vedaldi, A., Torr, P.H.S.: Fully-convolutional siamese networks for object tracking. In: Hua, G., Jégou, H. (eds.) *Computer Vision - ECCV 2016 Workshops - Amsterdam, The Netherlands, October 8-10 and 15-16, 2016, Proceedings, Part II. Lecture Notes in Computer Science*, vol. 9914, pp. 850–865 (2016)
2. Bhat, G., Danelljan, M., Gool, L.V., Timofte, R.: Learning discriminative model prediction for tracking. In: *2019 IEEE/CVF International Conference on Computer Vision, ICCV 2019, Seoul, Korea (South), October 27 - November 2, 2019*. pp. 6181–6190. IEEE (2019)
3. Chen, Z., Zhong, B., Li, G., Zhang, S., Ji, R.: Siamese box adaptive network for visual tracking. *CoRR* **abs/2003.06761** (2020), <https://arxiv.org/abs/2003.06761>
4. Dai, J., Qi, H., Xiong, Y., Li, Y., Zhang, G., Hu, H., Wei, Y.: Deformable convolutional networks. In: *IEEE International Conference on Computer Vision, ICCV 2017, Venice, Italy, October 22-29, 2017*. pp. 764–773. IEEE Computer Society (2017)
5. Danelljan, M., Bhat, G., Khan, F.S., Felsberg, M.: ECO: efficient convolution operators for tracking. In: *2017 IEEE Conference on Computer Vision and Pattern Recognition, CVPR 2017, Honolulu, HI, USA, July 21-26, 2017*. pp. 6931–6939. IEEE Computer Society (2017)
6. Danelljan, M., Bhat, G., Khan, F.S., Felsberg, M.: ATOM: accurate tracking by overlap maximization. In: *IEEE Conference on Computer Vision and Pattern Recognition, CVPR 2019, Long Beach, CA, USA, June 16-20, 2019*. pp. 4660–4669. Computer Vision Foundation / IEEE (2019)
7. Danelljan, M., Häger, G., Khan, F.S., Felsberg, M.: Learning spatially regularized correlation filters for visual tracking. In: *2015 IEEE International Conference on Computer Vision, ICCV 2015, Santiago, Chile, December 7-13, 2015*. pp. 4310–4318. IEEE Computer Society (2015)
8. Guo, D., Wang, J., Cui, Y., Wang, Z., Chen, S.: Siamcar: Siamese fully convolutional classification and regression for visual tracking. *CoRR* **abs/1911.07241** (2019), <http://arxiv.org/abs/1911.07241>
9. He, K., Zhang, X., Ren, S., Sun, J.: Deep residual learning for image recognition. In: *2016 IEEE Conference on Computer Vision and Pattern Recognition, CVPR 2016, Las Vegas, NV, USA, June 27-30, 2016*. pp. 770–778. IEEE Computer Society (2016)
10. Held, D., Thrun, S., Savarese, S.: Learning to track at 100 FPS with deep regression networks. In: Leibe, B., Matas, J., Sebe, N., Welling, M. (eds.) *Computer Vision - ECCV 2016 - 14th European Conference, Amsterdam, The Netherlands, October 11-14, 2016, Proceedings, Part I. Lecture Notes in Computer Science*, vol. 9905, pp. 749–765. Springer (2016)
11. Henriques, J.F., Caseiro, R., Martins, P., Batista, J.: High-speed tracking with kernelized correlation filters. *IEEE Transactions on Pattern Analysis and Machine Intelligence* **37**(3), 583–596 (2015)
12. Huang, L., Zhao, X., Huang, K.: Got-10k: A large high-diversity benchmark for generic object tracking in the wild. *IEEE Transactions on Pattern Analysis and Machine Intelligence* p. 11 (2019)
13. Kristan, M., Berg, A., Zheng, L., Rout, L., Gool, L.V., Bertinetto, L., Danelljan, M., Dunnhofer, M., Ni, M., Kim, M.Y., Tang, M., Yang, M., et al.: The seventh visual object tracking VOT2019 challenge results. In: *2019 IEEE/CVF International*

- Conference on Computer Vision Workshops, ICCV Workshops 2019, Seoul, Korea (South), October 27-28, 2019. pp. 2206–2241. IEEE (2019)
14. Kristan, M., Leonardis, A., Matas, J., Felsberg, M., Pflugfelder, R.P., Zajc, L.C., Vojír, T., Bhat, G., Lukezic, A., Eldesokey, A., Fernández, G., et al.: The sixth visual object tracking VOT2018 challenge results. In: Leal-Taixé, L., Roth, S. (eds.) *Computer Vision - ECCV 2018 Workshops - Munich, Germany, September 8-14, 2018, Proceedings, Part I. Lecture Notes in Computer Science*, vol. 11129, pp. 3–53. Springer (2018)
 15. Li, B., Wu, W., Wang, Q., Zhang, F., Xing, J., Yan, J.: Siamrpn++: Evolution of siamese visual tracking with very deep networks. In: *IEEE Conference on Computer Vision and Pattern Recognition, CVPR 2019, Long Beach, CA, USA, June 16-20, 2019*. pp. 4282–4291. Computer Vision Foundation / IEEE (2019)
 16. Li, B., Yan, J., Wu, W., Zhu, Z., Hu, X.: High performance visual tracking with siamese region proposal network. In: *2018 IEEE Conference on Computer Vision and Pattern Recognition, CVPR 2018, Salt Lake City, UT, USA, June 18-22, 2018*. pp. 8971–8980. IEEE Computer Society (2018)
 17. Li, Y., Zhu, J.: A scale adaptive kernel correlation filter tracker with feature integration. In: *Computer Vision - ECCV 2014 Workshops - Zurich, Switzerland, September 6-7 and 12, 2014, Proceedings, Part II. Lecture Notes in Computer Science*, vol. 8926, pp. 254–265. Springer (2014)
 18. Li, Y., Zhu, J., Hoi, S.C.H., Song, W., Wang, Z., Liu, H.: Robust estimation of similarity transformation for visual object tracking. In: *The Thirty-Third AAAI Conference on Artificial Intelligence, AAAI 2019, The Thirty-First Innovative Applications of Artificial Intelligence Conference, IAAI 2019, The Ninth AAAI Symposium on Educational Advances in Artificial Intelligence, EAAI 2019, Honolulu, Hawaii, USA, January 27 - February 1, 2019*. pp. 8666–8673. AAAI Press (2019)
 19. Lin, T., Goyal, P., Girshick, R.B., He, K., Dollár, P.: Focal loss for dense object detection. In: *IEEE International Conference on Computer Vision, ICCV 2017, Venice, Italy, October 22-29, 2017*. pp. 2999–3007. IEEE Computer Society (2017)
 20. Lin, T., Maire, M., Belongie, S.J., Hays, J., Perona, P., Ramanan, D., Dollár, P., Zitnick, C.L.: Microsoft COCO: common objects in context. In: Fleet, D.J., Pajdla, T., Schiele, B., Tuytelaars, T. (eds.) *Computer Vision - ECCV 2014 - 13th European Conference, Zurich, Switzerland, September 6-12, 2014, Proceedings, Part V. Lecture Notes in Computer Science*, vol. 8693, pp. 740–755. Springer (2014)
 21. Lukezic, A., Matas, J., Kristan, M.: D3S - A discriminative single shot segmentation tracker. CoRR [abs/1911.08862](https://arxiv.org/abs/1911.08862) (2019), <http://arxiv.org/abs/1911.08862>
 22. Lukezic, A., Vojír, T., Zajc, L.C., Matas, J., Kristan, M.: Discriminative correlation filter tracker with channel and spatial reliability. *Int. J. Comput. Vis.* **126**(7), 671–688 (2018)
 23. Ma, C., Huang, J., Yang, X., Yang, M.: Hierarchical convolutional features for visual tracking. In: *2015 IEEE International Conference on Computer Vision, ICCV 2015, Santiago, Chile, December 7-13, 2015*. pp. 3074–3082. IEEE Computer Society (2015)
 24. Ma, Z., Lu, W., Yin, J., Zhang, X.: Robust visual tracking via hierarchical convolutional features-based sparse learning. In: *10th International Conference on Wireless Communications and Signal Processing, WCSP 2018, Hangzhou, China, October 18-20, 2018*. pp. 1–7. IEEE (2018)
 25. Real, E., Shlens, J., Mazzocchi, S., Pan, X., Vanhoucke, V.: Youtube-boundingboxes: A large high-precision human-annotated data set for object detection in video. In: *2017 IEEE Conference on Computer Vision and Pattern Recog-*

- dition, CVPR 2017, Honolulu, HI, USA, July 21-26, 2017. pp. 7464–7473. IEEE Computer Society (2017)
26. Russakovsky, O., Deng, J., Su, H., Krause, J., Satheesh, S., Ma, S., Huang, Z., Karpathy, A., Khosla, A., Bernstein, M.S., et al.: Imagenet large scale visual recognition challenge. *International Journal of Computer Vision* **115**(3), 211–252 (2015)
 27. Sun, C., Wang, D., Lu, H., Yang, M.: Correlation tracking via joint discrimination and reliability learning. In: 2018 IEEE Conference on Computer Vision and Pattern Recognition, CVPR 2018, Salt Lake City, UT, USA, June 18-22, 2018. pp. 489–497. IEEE Computer Society (2018)
 28. Voigtlaender, P., Luiten, J., Torr, P.H.S., Leibe, B.: Siam R-CNN: visual tracking by re-detection. *CoRR* **abs/1911.12836** (2019), <http://arxiv.org/abs/1911.12836>
 29. Wang, Q., Zhang, L., Bertinetto, L., Hu, W., Torr, P.H.S.: Fast online object tracking and segmentation: A unifying approach. In: IEEE Conference on Computer Vision and Pattern Recognition, CVPR 2019, Long Beach, CA, USA, June 16-20, 2019. pp. 1328–1338. Computer Vision Foundation / IEEE (2019)
 30. Wu, Y., Lim, J., Yang, M.: Object tracking benchmark. *IEEE Trans. Pattern Anal. Mach. Intell.* **37**(9), 1834–1848 (2015)
 31. Xu, N., Yang, L., Fan, Y., Yang, J., Yue, D., Liang, Y., Price, B.L., Cohen, S., Huang, T.S.: Youtube-vos: Sequence-to-sequence video object segmentation. In: Ferrari, V., Hebert, M., Sminchisescu, C., Weiss, Y. (eds.) *Computer Vision - ECCV 2018 - 15th European Conference, Munich, Germany, September 8-14, 2018, Proceedings, Part V. Lecture Notes in Computer Science*, vol. 11209, pp. 603–619. Springer (2018)
 32. Xu, Y., Wang, Z., Li, Z., Ye, Y., Yu, G.: Siamfc++: Towards robust and accurate visual tracking with target estimation guidelines. *CoRR* **abs/1911.06188** (2019), <http://arxiv.org/abs/1911.06188>
 33. Yang, Z., Liu, S., Hu, H., Wang, L., Lin, S.: Reppoints: Point set representation for object detection. In: 2019 IEEE/CVF International Conference on Computer Vision, ICCV 2019, Seoul, Korea (South), October 27 - November 2, 2019. pp. 9656–9665. IEEE (2019)
 34. Yang, Z., Xu, Y., Xue, H., Zhang, Z., Urtasun, R., Wang, L., Lin, S., Hu, H.: Dense reppoints: Representing visual objects with dense point sets. *CoRR* **abs/1912.11473** (2019)
 35. Yu, Y., Xiong, Y., Huang, W., Scott, M.R.: Deformable siamese attention networks for visual object tracking. *CoRR* **abs/2004.06711** (2020), <https://arxiv.org/abs/2004.06711>
 36. Zhang, Z., Peng, H.: Deeper and wider siamese networks for real-time visual tracking. In: IEEE Conference on Computer Vision and Pattern Recognition, CVPR 2019, Long Beach, CA, USA, June 16-20, 2019. pp. 4591–4600. Computer Vision Foundation / IEEE (2019)
 37. Zhou, J., Wang, P., Sun, H.: Discriminative and robust online learning for siamese visual tracking. *CoRR* **abs/1909.02959** (2019), <http://arxiv.org/abs/1909.02959>
 38. Zhu, Z., Wang, Q., Li, B., Wu, W., Yan, J., Hu, W.: Distractor-aware siamese networks for visual object tracking. In: Ferrari, V., Hebert, M., Sminchisescu, C., Weiss, Y. (eds.) *Computer Vision - ECCV 2018 - 15th European Conference, Munich, Germany, September 8-14, 2018, Proceedings, Part IX. Lecture Notes in Computer Science*, vol. 11213, pp. 103–119. Springer (2018)